a-IGZO TFT-Based Selective Scan Driver with Stable Operation in Depletion Mode

Won-Been Jeong, Su-Hyeong Kim*, Seung-Won Kwak*, Hoon-Ju Chung**, and Seung-Woo Lee**

* Dept. of Information Display, Kyung Hee University, Seoul 02447, Korea
**School of Electronic Eng., Kumoh National Institute of Technology, Gumi, Gyeongbuk, 39177, Korea

Abstract

Increasing refresh rates and resolution elevate the operational frequency of scan drivers, leading to higher power consumption. The variable refresh rate (VRR) technique dynamically adjusts the refresh rate to reduce power consumption. However, VRR control the refresh rate for the entire area uniformly, which limits the potential to optimize power consumption. To address this limitation, an amorphous indium-gallium-zinc-oxide thin-film transistor (a-IGZO TFT)-based selective driving circuit was presented. This circuit reduces power consumption by allowing only selected areas to operate at a higher refresh rate. However, the proposed circuit cannot operate in depletion mode. This study proposes a selective driving circuit that supports selective driving while operating stably in both depletion and enhancement modes. Simulation results confirm the robustness of the proposed circuit against threshold voltage variations. This advancement can be applied to smartphone and virtual reality displays, enhancing power efficiency and delivering a high-quality user experience.

Author Keywords

a-IGZO TFT; Selective Driving; Depletion Mode; Power Efficiency;

1. Introduction

High resolution and high refresh rates are critical features in mobile displays, particularly for video content where smoother transitions and enhanced visual quality are essential [1, 2]. However, increasing refresh rates significantly raises the operational frequency of scan drivers, resulting in higher power consumption. This challenge is particularly severe in mobile devices, where limited battery capacity demands innovative solutions to improve power efficiency without compromising performance.

One promising solution to this challenge is the variable refresh rate (VRR) technique, which dynamically adjusts the refresh rate based on content type [3, 4]. For dynamic content, the display is refreshed at a higher rate to ensure smooth motion, while for static content, the rate is lowered. While VRR achieves power savings, the refresh rate is adjusted across the entire display. As a result, even when static and dynamic areas coexist within video content, the refresh rate must be selected for the dynamic content, leading to unnecessary power consumption.

To address this limitation, we proposed a selective scan driver circuit based on an amorphous indium-gallium-zinc-oxide thin-film transistor (a-IGZO TFT) [5]. By dividing the display into dynamic and static areas, this approach enables high refresh rates in dynamic areas while operating static areas at lower refresh rates. As illustrated in Fig. 1, the proposed circuit uses memory to adjust the scan driver inputs. The circuit generates output pulses for dynamic content and blocks them for static content. However, the proposed circuit is incompatible with depletion mode. This presents a critical limitation, as a-IGZO TFTs often exhibit significant threshold voltage (V_{TH}) variations [6-8], necessitating stable operation in both depletion and enhancement modes.

In this study, we propose a selective scan driver that ensures stable operation even in depletion mode. By addressing the challenges of depletion mode compatibility and threshold voltage variations, the proposed circuit provides a practical solution for integration into advanced display systems.

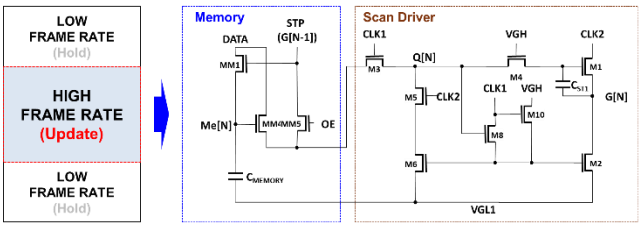

Figure 1. Concept of selective driving and our previously proposed selective driving circuit [5].

2. Proposed circuits

Fig. 2 presents our proposed circuit and timing diagram of signals for selective driving from G[N] to G[N+4]. The circuit consists of a memory unit and a scan driver unit, ensuring stable operation in depletion mode by employing a serially-connected two transistor (STT) structure [9] and a lower negative power level, VGL2 [10]. OE and DATA serve as global signals. The low voltage levels for CLKL1, CLKL2, and OE are set to VGL2, while the low voltage levels for CLK1, CLK2, and DATA are set to VGL1. The memory unit stores information for selective driving using a capacitor (C_{MEMORY}). We adopted a conventional scan driver circuit [11], which can be replaced with other compatible scan drivers.

The circuit operates in two modes: ordinary mode and selective driving mode. In ordinary mode, OE keeps its high voltage while DATA remains its low voltage, as the operation of a conventional scan driver. In selective driving mode, OE and DATA signals change based on the selected lines, enabling the higher refresh rate operation only in the selected area.

(a) Programming Period

During programming period, the scan driver generates sequential pulses while simultaneously storing selective driving information into the memory. After start pulse (STP) is initially generated, scan signals are produced sequentially as the scan driver operates. OE remains high, allowing the scan driver to function as a conventional driver. If G[N] is the first line to be selected to driven at higher refresh rate, DATA is adjusted to

ISSN 0097-996X/25/5601-0067-$1.00 © 2025

ensure that Me[N] becomes high.

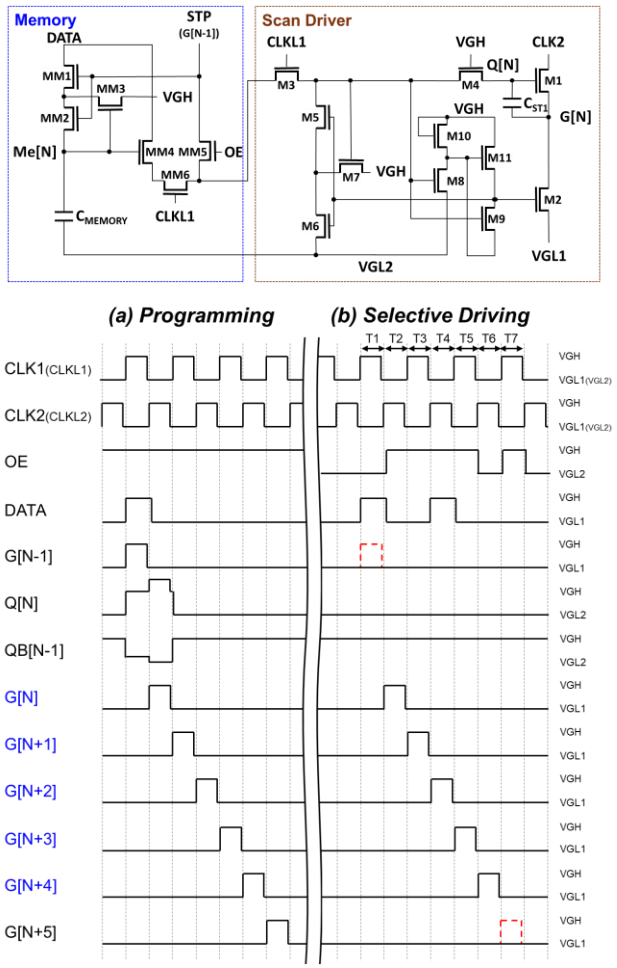

Figure 2. Circuit and timing diagram of signals for the proposed selective driving circuit

(b) Selective Driving Period

During selective driving period, STP keeps its low voltage, and the scan drivers from the first stage to the (n-1)th stage do not operate or produce output waveforms. While scan drivers do not operate, the voltage of OE remains low.

At T1, as DATA goes to high, Q[N] is charged to high voltage because Me[N] is high. Although Me[N+3] is also high, Q[N+3] is not charged because CLKL2 is low, as shown in Fig. 3(a). During this period, OE maintains its low voltage to block propagating from DATA to G[N-1].

At T2, when CLK2 goes to high, G[N] is generated, and OE goes to high, enabling Q[N+1] to be charged to the high voltage. At T3, OE remains high, allowing subsequent waveform to be generated.

At T4, when G[N+2] becomes high, DATA moves to high, ensuring that Me[N+3] stores high voltage. Although the voltage of Me[N] is high, Q[N] is not charged because CLKL1 remains low. At T5, G[N+3] is generated.

At T6, when G[N+4] is generated, OE goes to low voltage, stopping from generating output pulses any more. In the proposed circuit, Q node is usually discharged to the previous output pulse. However, with OE at a low voltage, Q[N+3] does not discharge to G[N+2]. Instead, due to the high voltage of Me[N+3] and the low voltage of DATA, Q[N+3] discharges through MM4 to the low voltage of DATA, as shown in Fig. 3(b). This driving scheme enables only the output waveforms of selected area to be generated at the high refresh rate. The total number of selected scan lines becomes odd because Q node is discharged through the previous scan line.

At T7, as OE goes to high, Q[N+4] is discharged to low. After T7, OE becomes low, since G[N-1] affects the low voltage level of Q[N].

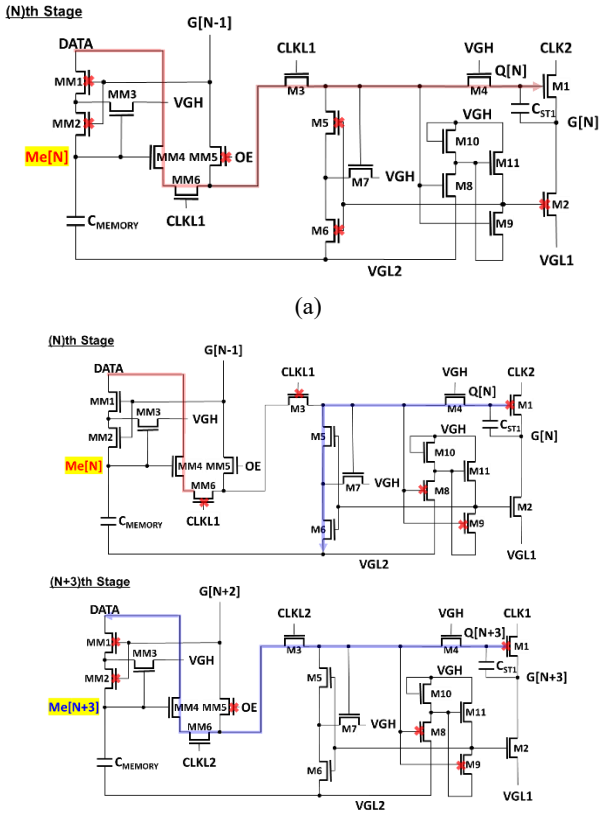

Figure 3. Detailed operation of the proposed selective driving circuit (a) at period T1 and (b) at period T6

3. Results and Discussion

To verify operation of the proposed circuit, we performed simulations. Fig. 4 presents the simulated and measured transfer characteristics of an a-IGZO TFT with a W/L of 3 μm/3 μm. The threshold voltage of TFT was -0.1 V, with a field-effect mobility of 12.5 $cm^2/V \cdot s$ and a subthreshold swing (S.S.) of 148 mV/dec. Table 1 summarizes the device and signal parameters used in the simulation. The simulations were conducted for a mobile display with a 1080×1920 resolution operating at a 120 Hz refresh rate, with the clock duty ratio of 40%.

Fig. 5 shows the simulation results of the proposed circuit for selective driving with 10 stages. In ordinary mode, all scan drivers operate at 120 Hz. In selective driving mode, the selected lines(G[5]-G[9]) operates at 120 Hz, while the other stages are driven at the lower refresh rates of 60 Hz or 30 Hz. The results demonstrate the proposed circuit can dynamically adjust refresh rates depending on the area.

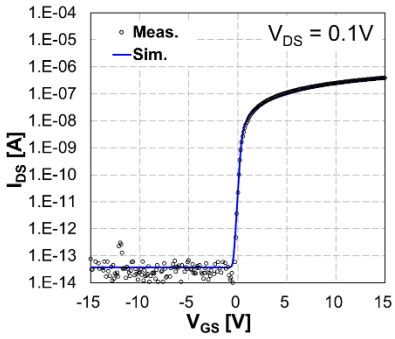

Figure 4. Measured and simulated transfer characteristics of a-IGZO TFT.

Table 1. Parameters of the proposed circuit

Parameters	Values	Parameters	Values
MM1-MM3, M5-M9	3 µm/3 µm	C_{Memory}	50 fF
MM4-MM6, M3, M4	12 µm/3 µm	*VGH*	10V
M10, M11	3 µm/12 µm	*VGL1*	−6V
M1	240 µm/3 µm	*VGL2*	−10V
M2	120 µm/3 µm	*Pulse width*	3.2 us
C_{ST}	200 fF	R_{Load}/C_{Load}	3 kΩ/20 pF

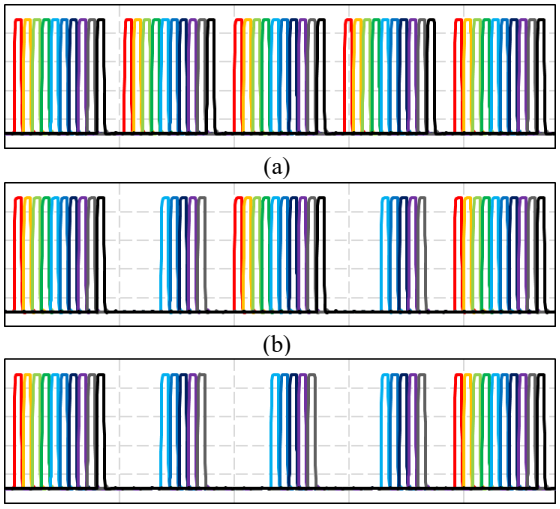

(a)

(b)

(c)

Figure 5. Simulation results of the proposed scan driver: (a) Ordinary mode at 120 Hz, (b) selective driving mode with 120 Hz and 60 Hz, and (c) selective driving mode with 120 Hz and 30 Hz.

Fig. 6 shows the simulation results of the proposed circuit under V_{TH} variations ranging from –2.0 V to +2.0 V. The selective driving waveforms were successfully generated in both modes, with portions of the selected region operating at 120 Hz. The rising times were approximately 167 ns and 183 ns, while the falling times were 169 ns and 183 ns for depletion mode and enhancement mode, respectively.

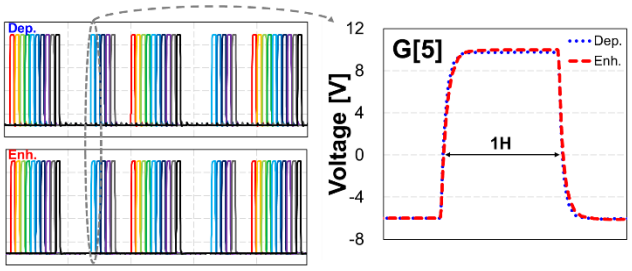

Figure 6. Simulation results of selective driving in depletion mode and enhancement mode (ΔV_{TH} = ±2.0V)

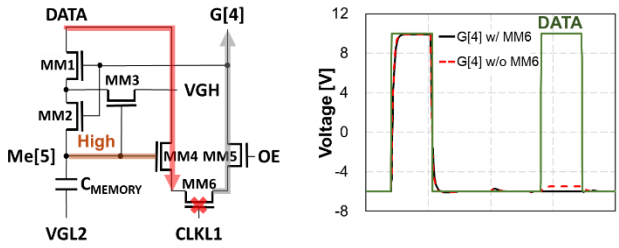

Figure 7. Impact of MM6 on preventing unintended propagation of DATA to G[4].

Fig. 7 illustrates how incorporating MM6 into the proposed circuit prevents the unintended propagation of DATA to G[4]. For the selective driving of G[5]-G[9], Me[5] and Me[8] are programmed to store high voltages. When DATA goes high for the second time to set Me[8] to a high voltage, Me[5] is already in a high state. Without MM6, DATA voltage could be transferred to G[4] through MM5, causing an unintended ripple of G[4]. The addition of MM6 blocks this unintended ripple of G[4], ensuring stable operation and reducing unnecessary power consumption.

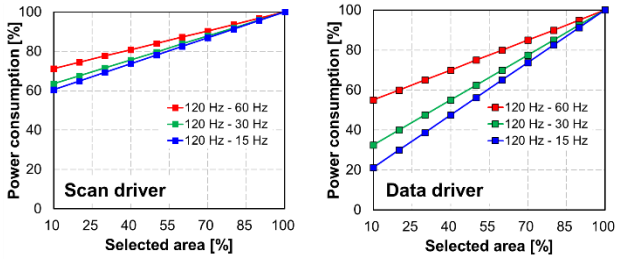

Figure 8. Power reduction achieved through selective driving

Fig. 8 depicts the power reduction achieved in selective driving mode compared to ordinary mode, based on the proportion of selectively driven areas and their respective refresh rates. The results demonstrate that lowering the refresh rate of selected area can effectively reduce power consumption of the scan driver. However, the power reduction in the scan driver is somewhat limited due to the power consumption associated with the CLK signals. Instead, more significant power savings can be achieved through the data driver, as the reduction in operating frequency plays a much more substantial role in minimizing power consumption. The power reduction of the scan driver in Fig. 8 is based on dynamic power calculations.

We believe that the proposed circuit can be effectively applied not only to mobile devices but also to virtual reality (VR) displays. VR displays continue to push toward higher resolution and higher refresh rates to enhance user experience. However, these improvements also lead to significantly increased power

consumption in the scan driver circuits. In our previous study [12], we conducted experiments in a VR environment and verified that applying selective driving technology allowed users to perceive image quality comparable to the original content. This demonstrates that the proposed circuit is capable of maintaining high visual fidelity while reducing power consumption in VR displays. Furthermore, when combined with eye-tracking technology, the proposed circuit can dynamically control DATA and OE signals to selectively drive selected area of the display based on the user's gaze. This approach not only optimizes power efficiency but also enables targeted high refresh rate operation in area that require enhanced visual performance, further improving the overall VR experience.

4. Conclusion

This study presents a power-efficient a-IGZO TFT-based selective scan driver circuit capable of stable operation in both depletion and enhancement modes. By selectively driving specific areas of the display at high refresh rates and maintaining lower refresh rates for other regions, the proposed circuit effectively reduces unnecessary power consumption with significant savings achieved particularly in the data driver. Simulations confirm the circuit's robustness under threshold voltage variations, overcoming a key limitation of previous circuits that lacks compatibility with depletion mode operation. These advancements make the circuit well-suited for applications in mobile and VR displays, balancing the demand for high resolution and refresh rates with strict power efficiency requirements.

5. Acknowledgements

This work was supported in part by the Technology Innovation Program (20016317, On-Panel Circuit Integration and Driving System Technology for 1270 ppi Low-Power OLED Display Based on Oxide Semiconductor) funded by the Ministry of Trade, Industry & Energy (MOTIE, Korea) and the EDA Tool was supported by the IC Design Education Center.

6. References

1. J. Wang, R. Shi, W. Zheng, W. Xie, D. Kao, and H.-N. Liang, "Effect of Frame Rate on User Experience, Performance, and Simulator Sickness in Virtual Reality," *IEEE Trans. Vis. Comput. Graphics*, vol. 29, no. 5, pp. 2478–2488, May 2023, doi: 10.1109/TVCG.2023.3247057.
2. Y.-H. Wu et al., "Breaking the Limits of Virtual Reality Display Resolution: The Advancements of a 2117-Pixels per Inch 4K Virtual Reality Liquid Crystal Display," *J. Opt. Microsystems*, vol. 3, no. 4, pp. 041208, 2023, doi: 10.1117/1.JOM.3.4.041208.
3. B. You, H. Nam, and H. Lee, "46-3: Image Adaptive Refresh Rate Technology for Ultra Low Power Consumption," *SID Symp. Dig. Tech. Papers*, vol. 51, no. 1, pp. 676–679, 2020, doi: 10.1002/sdtp.13958.
4. G. A. Slavenburg, M. Janssens, L. Lucas, R. J. Schutten, and T. Verbeure, "46-1: Invited Paper: Variable Refresh Rate Displays," *SID Symp. Dig. Tech. Papers*, vol. 51, no. 1, pp. 669–672, 2020, doi: 10.1002/sdtp.13956.
5. J.-H. Jo, W.-B. Jeong, Y.-S. Joung, and S.-W. Lee, "Selective Scan Driver for Low-Power Consumption Using Oxide Thin Film Transistors," *IEEE Electron Device Lett.*, vol. 43, no. 8, pp. 1263–1266, Aug. 2022, doi: 10.1109/LED.2022.3184337.
6. B. Kim et al., "Highly Reliable Depletion-Mode a-IGZO TFT Gate Driver Circuits for High-Frequency Display Applications Under Light Illumination," *IEEE Electron Device Lett.*, vol. 33, no. 4, pp. 528–530, Apr. 2012, doi: 10.1109/LED.2011.2181969.
7. T.-Y. Hsieh et al., "Investigation of Gate-Bias Stress and Hot-Carrier Stress-Induced Instability of InGaZnO Thin-Film Transistors Under Different Environments," *Surf. Coat. Technol.*, vol. 231, pp. 478–481, 2013, doi: 10.1016/j.surfcoat.2012.10.030.
8. J. Cho et al., "Gate Bias Stress Reliability of a-InGaZnO TFTs Under Various Channel Dimensions," *Microelectron. Rel.*, vol. 153, p. 115308, 2024, doi: 10.1016/j.microrel.2023.115308.
9. B. Kim et al., "A Depletion-Mode a-IGZO TFT Shift Register With a Single Low-Voltage-Level Power Signal," *IEEE Electron Device Lett.*, vol. 32, no. 8, pp. 1092–1094, Aug. 2011, doi: 10.1109/LED.2011.2157989
10. B. Kim et al., "New Depletion-Mode IGZO TFT Shift Register," *IEEE Electron Device Lett.*, vol. 32, no. 2, pp. 158–160, Feb. 2011, doi: 10.1109/LED.2010.2090939.
11. D.-S. Kim and O.-K. Kwon, "A Small-Area and Low-Power Scan Driver Using a Coplanar a-IGZO Thin-Film Transistor With a Dual-Gate for Liquid Crystal Displays," *IEEE Electron Device Lett.*, vol. 38, no. 2, pp. 195–198, Feb. 2017, doi: 10.1109/LED.2016.2638832.
12. W.-B. Jeong and S.-W. Lee, "Gaze-Dependent Refresh W.-B. Jeong and S.-W. Lee, "Gaze-Dependent Refresh Technique for a Low-Power VR System," in *Proc. IEEE Int. Conf. Consumer Electron. (ICCE)*, 2024, pp. 1–4, doi: 10.1109/ICCE59016.2024.10444491.